

Ultrasensitive impedimetric immunosensor for the detection of C-reactive protein in blood at *SI-RAFT* generated pHEMA brushes

Prosper Kanyong[†], Candan Catli[†] and Jason J. Davis^{†,*}.

Department of Chemistry, University of Oxford, South Parks Road, Oxford OX1 3TA, UK.

ABSTRACT: The reversible addition-fragmentation chain transfer (*RAFT*) polymerization of 2-hydroxyethyl methacrylate (HEMA) from a surface confined, dithio-tethered, chain transfer agent (CTA) enables the preparation of electrode-tethered poly (2-hydroxyethyl methacrylate) (pHEMA) brushes of well-defined thickness with convenience and exceptionally high interfacial impedimetric baseline stability. The subsequent covalent integration of antibodies generates interfaces of very high target recognition specificity, ultimately enabling fM levels of quantification of C-reactive protein (CRP) and recovery in spiked serum samples of ~98%. When combined with the intrinsic scalability of the reagentless EIS platform and the innate high levels of polymer tuneability and control, we believe this represents a valuable contribution to the diagnostic toolbox.

The sensitive and selective detection of protein biomarkers plays a vital role in the diagnosis of infection, a range of disease states, and general assessments of trauma¹. Progress along this road will undoubtedly advance disease stratification, early diagnosis and the assessment of treatment efficacy². A routine use of existing methodologies for high-throughput, point-of-care testing has however, been severely hampered by the slow, cumbersome and somewhat error-prone standard methods for protein assaying such as those based on multistep immunoassays, mass spectroscopy, or turbidimetric analyses³. Of the range of methods available, those which are label-free bring advantages associated with decreased cost and sample preparation and assay time and eliminate the potentially perturbative effects of chemical labelling⁴. However, label-free assays generally considered to be less sensitive/less amplified than labelled equivalents and are prone to potentially profoundly detrimental non-specific signals from bio-fouling⁵. Coupled with the knowledge that a significant amount of disease biomarkers are present in biological fluids (a complex matrix) and sometimes at extremely low (picomolar or even femtomolar) levels⁶, it is imperative that progress is made in maximizing sensitivity whilst retaining selectivity in real samples (such as blood, urine and saliva) if such methods are to be applicable to, for example, near-patient clinical diagnostics. A key aspect of such sensors, in this regard, is their fouling and the development of effective anti-fouling interfaces that resist protein adsorption requires not only a design of materials of appropriate intrinsic chemical character (e.g. hydrophilicity and net charge) but also good levels of control over its physicochemical characteristics once surface integrated (e.g. film thickness, packing density and surface roughness)⁷. Among the hydrophilic anti-fouling materials, poly(ethylene glycol)(PEG)-based self-assembled monolayers are, in particular well known; thus, they have been widely used within sensors interfaces^{8,9}. However, PEG-based oligomers are readily subject to oxidation in complex media such as blood plasma and serum and are also not able to withstand fouling in very competitive media such as serum¹⁰. Under such conditions zwitterionic polymers such as poly(carboxybeta-

ine)(pCB) have been shown, in recent years, to be more effective where hydration layers, chain mobility, and exclusion volumes all contribute significantly to the anti-fouling characteristics¹¹. The synthetic routes available to these interfaces can be problematic as can be structure based predictions on performance (given the variable contributions of electrostatic and hydrogen bonded hydrations). Hydrophilic and uncharged polymeric interfaces, such as those based on 2-hydroxyethyl methacrylate (HEMA), *N*-hydroxyethyl acrylamide (HEAA), and *N*-acryloylaminoethoxyethanol (AAEE), have also been shown to reduce biofouling substantially¹². A range of polymeric materials incorporating HEMA have been developed for application in contact lenses, dental fillings, surgical implants, tissue engineering scaffolds, catheters, hemodialysis membranes, wound dressings and drug delivery systems¹³. These are generally prepared by traditional free radical polymerization techniques¹⁴ not conducive to the formation of well-defined polymer brushes and have not been prior utilized in selective electrochemical assays^{15,16}.

Living polymerization methods are much more suitable¹⁷ if one seeks good levels of control over parameters that are important in downstream sensor behavior, namely brush thicknesses, composition, and architecture¹⁸. The methods available for this are nitroxide mediated polymerization (NMP), atom transfer radical polymerization (ATRP) and reversible addition-fragmentation chain transfer (RAFT) polymerization^{17,19,20}. However, NMP typically requires high temperatures not readily translatable to thin film growth, while ATRP requires the use of a surface tethered tertiary halide initiator and cytotoxic metal catalysts²¹. RAFT is a versatile technique for controlled radical polymerization which does not require the use of toxic catalysts²² and is applicable to a wide range of monomers including well-known non-fouling monomers such as betaines and hydroxyl-functional methacrylamido monomers^{22,23}. There are three approaches for conducting a surface-initiated RAFT (*SI-RAFT*) polymerization (that would generate a surface tethered functional polymer) depending on the type of species anchored to the substrate: (i) initiator, (ii) chain transfer agent (CTA) via

the Z-group and, (iii) CTA via the R-group. Among these approaches, CTA via the R-group is the most promising methods for preparing well-defined polymer brushes with a low PDI ²⁴. The main drawbacks associated with these methods is that all of them require the initial presence of a well-packed self-assembled monolayer (SAM) with end-groups to which an initiator or RAFT agent can be coupled. To overcome these problems, we have herein utilized a facile strategy for the *SI*-RAFT polymerization of HEMA using 4-cyano-4-(phenylcarbonothioylthio)pentanoic acid as CTA, grafted directly via its dithio-group to the surface of gold substrates. This approach was developed with the aim of designing well-defined pHEMA brushes with controlled thickness from the CTA agent generated SAM, without the need to recourse to a RAFT agent with specific functional Z-/R-group and/or catalysts. In this “grafting from” approach, the polymerization is directly initiated from CTA-functionalized surface.

The prepared pHEMA brushes were characterized in detail and challenged with proteins and serum and their resistance to fouling monitored by electrochemical impedance spectroscopy (EIS). The subsequent receptor modification of these brushes led to interfaces of very high signal stability and target specific impedimetric sensors with a remarkably low detection limit. The practical capability of the immunosensor was validated through the quantification of CRP in buffer and recovery of CRP spiked into serum samples.

CTA chemisorbs robustly on clean gold electrodes to present an adlayer with a high barrier to electron transfer as expected²⁵ and ATR-IR signatures as discussed below. The subsequent synthesis of the pHEMA brushes were prepared by surface-initiated (*SI*) reversible addition-fragmentation chain-transfer (*SI*-RAFT) of 2-hydroxyethyl methacrylate (HEMA) monomers and were characterized by contact angle analysis, FTIR-ATR and atomic force microscopy (AFM), with brush thicknesses tuned across the 2.0 to 50 nm range by changing polymerization time. Figure S1 shows contact angles of bare and CTA-coated Au and the generated pHEMA brush of $\sim 10.0 \text{ nm} \pm 2.0$ thickness (that resolved to be most appropriate for impedimetric analyses – see below) where these are observed to change from 78.5° on bare Au, to 75.5° on the CTA-coated Au and further reduced to 34.3° on pHEMA-grafted Au, a presented hydrophilicity that is consistent with prior reports^{26,27}. FTIR-ATR spectra of these interfaces resolved modes as expected (Figure S2). AFM topography scans for Au, and dry films of CTA, pHEMA-CTA and CRP-anti-CRP-pHEMA-CTA samples were evaluated and a cross-sectional analysis of the root-mean-square (RMS) of dry film roughness was estimated to be $\sim 5.8 \text{ nm}$ (for CRP-anti-CRP-pHEMA-CTA), indicative of a homogeneous polymer brush^{28,29}.

The fouling of these brush interfaces by neat fetal bovine serum (FBS) and 5% FBS (Section 2.1) was quantified (Figure 1a) through resolved changes in impedimetric R_{ct} after two hours of incubation. There were resolved mean increases in R_{ct} of $\sim 30\% \pm 1.3$ $\sim 10\% \pm 1.1$ and $\sim 4\% \pm 1.8$ for brushes of 2.5 nm, 10 nm, and 20 nm respectively. Although this trend is in line with expectations, subsequent antibody modification of the thickness (20 nm) brushes led to R_{ct} values that were prohibitively high and not reliably responsive to specific target capture thereafter. Consequently, the 10 nm brush interface was deemed the most effective compromise and used throughout the remainder of this study.

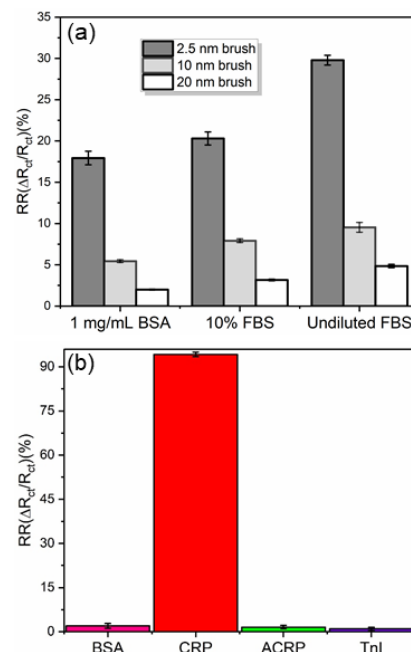


Figure 1: (a) Relative response (RR, % for the adsorption of bovine serum albumin (BSA, 1000.0 mg/L) and different percentages of fetal bovine serum (FBS) tested using the pHEMA brushes; (b) Selectivity of AulCTA/pHEMA/anti-CRP immunosensor to bovine serum albumin (BSA, 1000.0 mg/L), C-reactive protein (CRP, 0.2 mg/L), anti-CRP (200.0 mg/L) and Troponin I (TnI, 0.2 mg/L). Error bars represent one standard deviation across three independent measurements (across different electrodes).

Electrochemical impedance spectroscopy, in its commonly applied Faradaic form, serves as a convenient and sensitive tool for assaying captured target biomarkers at an appropriately functionalized electrode interface. However, the necessary use of relatively high level of solution redox species, though signal amplifying, can present challenges with respect to baseline signal stability that need to be prior screened if any downstream assay is to be deemed reliable^{30,31}. The 10 nm pHEMA brushes generated herein were incubated in PBS (10.0 mM, pH 7.4) and Faradaic EIS analyses carried out at regular time intervals for up to 24 days (Figure S3). The R_{ct} drifted of less than 2.0 % across this period is indicative of quite exceptional baseline stability³².

The selectivity of the immunosensor was evaluated by exposure to clinically relevant levels of troponin I (TnI), bovine serum albumin (BSA), C-reactive protein (CRP) and anti-CRP (Figure 1b) where the resolved R_{ct} signal changes were $\sim 2\% \pm 1.2$, $\sim 1\% \pm 1.4$ and $\sim 1.5 \pm 1.1$ % respectively. By way of comparison, the same sensor interfaces respond to $1.75 \mu\text{M}$ target (CRP) with a $> 94\%$ signal change. The sensors respond in a log linear manner to CRP across its entire clinically relevant range (Figures 2a and 2b) with data fitting well ($R^2 = 0.996$) to a simple Langmuir adsorption model (Figure S4) that resolves an associated (K_d) as 13 nM. CRP has been routinely analyzed using ELISA, immunoturbidimetry and antibody-based nephelometric assays; these are usually sensitive to concentrations of 5 – 20 mg/L. However, recent realization of the utility of accurate (true and precise) measurement of CRP as a prognostic risk biomarker of cardiovascular disease has led to the development of high-sensitivity CRP (hs-CRP) assays to

detect lower levels in 0.5 – 10 mg/L range^{33,34}. A serum CRP threshold of <5 mg/L was suggested by the World Health Organization to define normal values when using a rapid diagnostic test or <3 – 10 mg/L when using immunoassays (e.g. ELISA)^{35,36}. The current turbidimetric and nephelometric assays do not cover these required measuring ranges. Beside this, a typical ELISA has LOD of ~1 ng/mL requiring ~4 hr to complete³⁷; this is similar to traditional analytical lab-based instruments such as the Hitachi 7600 Chemistry Analyzers. The associated detection limit of the sensor developed herein ($3\sigma/S$, where σ is the standard deviation of the background signal and S is the slope of the linear calibration) of $7.02 \text{ ng/L} \pm 1.57$ (~62 fM) is exceptionally low for an unamplified label free analysis. These characteristics are notably superior to any prior CRP based impedance sensor, (Table S1) and the assay itself can be completed within few minutes. The electrochemical format is also reagentless, single step and readily integrated into both automated fluid handlers and multiplex formats with retention of assay specificity.

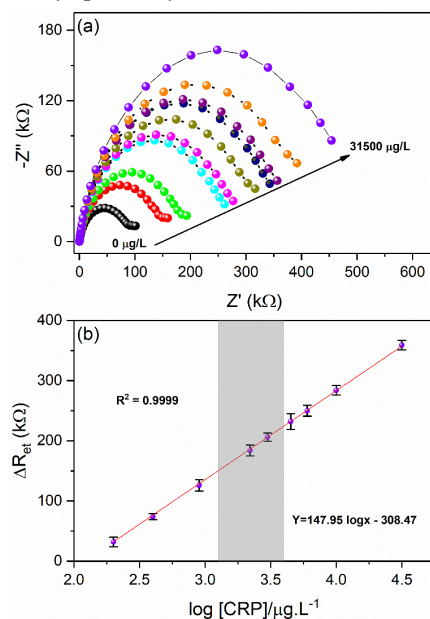


Figure 2. (a) Nyquist plots for Au/CTA/pHEMA/anti-CRP at various concentrations of CRP ranging from 0 to 31500 µg/L; and the (b) corresponding calibration curve of the immunosensor for the detection of CRP; the grey shaded area indicates the clinically relevant range for cardiac disease. Error bars represent one standard deviation across three independent measurements (across different electrodes).

FEIS, with multiple standard additions³⁸ (Figure S5), was used to recover CRP (0.9 mg/L) spiked into FBS (5%), with incubations of 15 min prior to Nyquist data acquisition (Figure S5a). Three replicate FBS samples were analyzed and the results (ΔR_{et}) were used to construct standard addition plots (Figure S5b). The means of these experimentally derived values were used to calculate the mean CRP recovery (the histogram in Figure S5c), 98% somewhat better than has been reported recently for this marker.^{39,40} Taken together with the detection sensitivity and high reagentless baseline stability, this demonstrates substantial promise for the analysis of real patient samples.

In this study, CTA was grafted via its dithio-group to the surface of Au electrodes prior to the thermally activated *SI-RAFT*

growth of pHEMA brushes of well-defined thickness. These hydrophilic films (2.5 nm to 20.0 nm thick) exhibit high levels of protein resistance and, significantly, exceptional impedimetric baseline stabilities. In combination these features support the reagentless detection of CRP down to exceptionally low levels with recoveries in serum that are highly encouraging of an extrapolation to real patient sample analysis (analytical features that exceed those of any prior reported electrochemical CRP sensors; Table S1).

ASSOCIATED CONTENT

Supporting Information

The Supporting Information is available free of charge on the ACS Publications website at DOI:

Materials and methods, characterization figures of sensor and supplementary data (PDF)

AUTHOR INFORMATION

Corresponding Author

* Email; jason.davis@chem.ox.ac.uk

Present Addresses

†Department of Chemistry, University of Oxford, South Parks Road, Oxford, OX1 3TA, UK.

Notes

The authors declare no competing financial interest.

ACKNOWLEDGMENT

The authors gratefully acknowledge the financial support (Grant Number DHR001130) given to this work by Osler Diagnostics.

REFERENCES

- (1) Bakirhan, N. K.; Ozcelikay, G.; Ozkan, S. A. Recent Progress on the Sensitive Detection of Cardiovascular Disease Markers by Electrochemical-Based Biosensors. *J. Pharm. Biomed. Anal.* **2018**, *159*, 406–424. <https://doi.org/https://doi.org/10.1016/j.jpba.2018.07.021>.
- (2) Swierczewska, M.; Liu, G.; Lee, S.; Chen, X. High-Sensitivity Nanosensors for Biomarker Detection. *Chem. Soc. Rev.* **2012**, *41* (7), 2641–2655. <https://doi.org/10.1039/C1CS15238F>.
- (3) Hortin, G. L.; Carr, S. A.; Anderson, N. L. Introduction: Advances in Protein Analysis for the Clinical Laboratory. *Clin. Chem.* **2010**, *56* (2), 149 LP – 151. <https://doi.org/10.1373/clinchem.2009.132803>.
- (4) Stern, E.; Vacic, A.; Rajan, N. K.; Criscione, J. M.; Park, J.; Ilic, B. R.; Mooney, D. J.; Reed, M. A.; Fahmy, T. M. Label-Free Biomarker Detection from Whole Blood. *Nat. Nanotechnol.* **2009**, *5*, 138.
- (5) Xu, Q.; Davis, J. J. The Diagnostic Utility of Electrochemical Impedance. *Electroanalysis* **2014**, *26* (6), 1249–1258. <https://doi.org/10.1002/elan.201400035>.
- (6) Etzioni, R.; Urban, N.; Ramsey, S.; McIntosh, M.; Schwartz, S.; Reid, B.; Radich, J.; Anderson, G.; Hartwell, L. The Case for Early Detection. *Nat. Rev. Cancer* **2003**, *3* (4), 243–252. <https://doi.org/10.1038/nrc1041>.
- (7) Chen, L.; Thérien-Aubin, H.; Wong, M. C. Y.; Hoek, E. M. V.; Ober, C. K. Improved Antifouling Properties of Polymer Membranes Using a ‘Layer-by-Layer’ Mediated Method. *J. Mater. Chem. B* **2013**, *1* (41), 5651–5658. <https://doi.org/10.1039/C3TB20916D>.
- (8) Zolk, M.; Eisert, F.; Pipper, J.; Herrwerth, S.; Eck, W.; Buck, M.; Grunze, M. Solvation of Oligo(Ethylene Glycol)-Terminated Self-Assembled Monolayers Studied by Vibrational Sum Frequency Spectroscopy. *Langmuir* **2000**, *16* (14), 5849–5852. <https://doi.org/10.1021/la0003239>.

- (9) Zheng, J.; Li, L.; Chen, S.; Jiang, S. Molecular Simulation Study of Water Interactions with Oligo (Ethylene Glycol)-Terminated Alkanethiol Self-Assembled Monolayers. *Langmuir* **2004**, *20* (20), 8931–8938. <https://doi.org/10.1021/la036345n>.
- (10) Zhang, Z.; Zhang, M.; Chen, S.; Horbett, T. A.; Ratner, B. D.; Jiang, S. Blood Compatibility of Surfaces with Superlow Protein Adsorption. *Biomaterials* **2008**, *29* (32), 4285–4291. <https://doi.org/https://doi.org/10.1016/j.biomaterials.2008.07.039>.
- (11) Chen, S.; Li, L.; Zhao, C.; Zheng, J. Surface Hydration: Principles and Applications toward Low-Fouling/Nonfouling Biomaterials. *Polymer (Guildf)*. **2010**, *51* (23), 5283–5293. <https://doi.org/https://doi.org/10.1016/j.polymer.2010.08.022>.
- (12) Serrano, Á.; Sterner, O.; Mieszkina, S.; Zürcher, S.; Tosatti, S.; Callow, M. E.; Callow, J. A.; Spencer, N. D. Nonfouling Response of Hydrophilic Uncharged Polymers. *Adv. Funct. Mater.* **2013**, *23* (46), 5706–5718. <https://doi.org/10.1002/adfm.201203470>.
- (13) Montheard, J.-P. P.; Chatzopoulos, M.; Chappard, D. 2-Hydroxyethyl Methacrylate (HEMA): Chemical Properties and Applications in Biomedical Fields. *J. Macromol. Sci. Part C* **1992**, *32* (1), 1–34. <https://doi.org/10.1080/15321799208018377>.
- (14) Fernández-García, M.; Torrado, M. F.; Martínez, G.; Sánchez-Chaves, M.; Madruga, E. L. Free Radical Copolymerization of 2-Hydroxyethyl Methacrylate with Butyl Methacrylate: Determination of Monomer Reactivity Ratios and Glass Transition Temperatures. *Polymer (Guildf)*. **2000**, *41* (22), 8001–8008. [https://doi.org/10.1016/S0032-3861\(00\)00167-1](https://doi.org/10.1016/S0032-3861(00)00167-1).
- (15) Tsarevsky, N. V.; Pintauer, T.; Matyjaszewski, K. Deactivation Efficiency and Degree of Control over Polymerization in ATRP in Protic Solvents. *Macromolecules* **2004**, *37* (26), 9768–9778. <https://doi.org/10.1021/ma048438x>.
- (16) Panzarasa, G.; Soliveri, G.; Pifferi, V. Tuning the Electrochemical Properties of Silicon Wafer by Grafted-from Micropatterned Polymer Brushes. *J. Mater. Chem. C* **2016**, *4* (2), 340–347. <https://doi.org/10.1039/C5TC03367E>.
- (17) Kakwere, H.; Perrier, S. Design of Complex Polymeric Architectures and Nanostructured Materials/Hybrids by Living Radical Polymerization of Hydroxylated Monomers. *Polym. Chem.* **2011**, *2* (2), 270–288. <https://doi.org/10.1039/C0PY00160K>.
- (18) Barbey, R.; Lavanant, L.; Paripovic, D.; Schüwer, N.; Sugnaux, C.; Tugulu, S.; Klok, H.-A. Polymer Brushes via Surface-Initiated Controlled Radical Polymerization: Synthesis, Characterization, Properties, and Applications. *Chem. Rev.* **2009**, *109* (11), 5437–5527. <https://doi.org/10.1021/cr900045a>.
- (19) Braunecker, W. A.; Matyjaszewski, K. Controlled/Living Radical Polymerization: Features, Developments, and Perspectives. *Prog. Polym. Sci.* **2007**, *32* (1), 93–146. <https://doi.org/https://doi.org/10.1016/j.progpolymsci.2006.11.002>.
- (20) Hawker, C. J.; Bosman, A. W.; Harth, E. New Polymer Synthesis by Nitroxide Mediated Living Radical Polymerizations. *Chem. Rev.* **2001**, *101* (12), 3661–3688. <https://doi.org/10.1021/cr990119u>.
- (21) Rizzardo, E.; Solomon, D. H. On the Origins of Nitroxide Mediated Polymerization (NMP) and Reversible Addition–Fragmentation Chain Transfer (RAFT). *Aust. J. Chem.* **2012**, *65* (8), 945. <https://doi.org/10.1071/ch12194>.
- (22) Pissuwan, D.; Boyer, C.; Gunasekaran, K.; Davis, T. P.; Bulmus, V. In Vitro Cytotoxicity of RAFT Polymers. *Biomacromolecules* **2010**, *11* (2), 412–420. <https://doi.org/10.1021/bm901129x>.
- (23) Rodríguez-Emmenegger, C.; Schmidt, B. V. K. J.; Sedlakova, Z.; Šubr, V.; Alles, A. B.; Brynda, E.; Barner-Kowollik, C. Low Temperature Aqueous Living/Controlled (RAFT) Polymerization of Carboxybetaine Methacrylamide up to High Molecular Weights. *Macromol. Rapid Commun.* **2011**, *32* (13), 958–965. <https://doi.org/10.1002/marc.201100176>.
- (24) Zhou, D.; Mastan, E.; Zhu, S. Termination of Surface Radicals and Kinetic Analysis of Surface-Initiated RAFT Polymerization on Flat Surfaces. *Macromol. Theory Simulations* **2012**, *21* (9), 602–614. <https://doi.org/10.1002/mats.201200043>.
- (25) Janek, R. P.; Fawcett, W. R.; Ulman, A. Impedance Spectroscopy of Self-Assembled Monolayers on Au(111): Sodium Ferrocyanide Charge Transfer at Modified Electrodes. *Langmuir* **1998**, *14* (11), 3011–3018. <https://doi.org/10.1021/la970980+>.
- (26) Zhao, C.; Li, L.; Wang, Q.; Yu, Q.; Zheng, J. Effect of Film Thickness on the Antifouling Performance of Poly(Hydroxy-Functional Methacrylates) Grafted Surfaces. *Langmuir* **2011**, *27* (8), 4906–4913. <https://doi.org/10.1021/la200061h>.
- (27) Fang, Y.; Xu, W.; Meng, X.-L.; Ye, X.-Y.; Wu, J.; Xu, Z.-K. Poly(2-Hydroxyethyl Methacrylate) Brush Surface for Specific and Oriented Adsorption of Glycosidases. *Langmuir* **2012**, *28* (37), 13318–13324. <https://doi.org/10.1021/la302738s>.
- (28) Desseaux, S.; Hineströsa, J. P.; Schüwer, N.; Lokitz, B. S.; Ankner, J. F.; Kilbey, S. M.; Voitchovsky, K.; Klok, H.-A. A. Swelling Behavior and Nanomechanical Properties of (Peptide-Modified) Poly(2-Hydroxyethyl Methacrylate) and Poly(Poly(Ethylene Glycol) Methacrylate) Brushes. *Macromolecules* **2016**, *49* (12), 4609–4618. <https://doi.org/10.1021/acs.macromol.6b00881>.
- (29) Bai, L.; Tan, L.; Chen, L.; Liu, S.; Wang, Y. Preparation and Characterizations of Poly(2-Methyl-2-Oxazoline) Based Antifouling Coating by Thermally Induced Immobilization. *J. Mater. Chem. B* **2014**, *2* (44), 7785–7794. <https://doi.org/10.1039/c4tb01383b>.
- (30) Flynn, N. T.; Tran, T. N. T.; Cima, M. J.; Langer, R. Long-Term Stability of Self-Assembled Monolayers in Biological Media. *Langmuir* **2003**, *19* (26), 10909–10915. <https://doi.org/10.1021/la035331e>.
- (31) Riepl, M.; Mirsky, V. M.; Novotny, I.; Tvarozek, V.; Rehacek, V.; Wolfbeis, O. S. Optimization of Capacitive Affinity Sensors: Drift Suppression and Signal Amplification. *Anal. Chim. Acta* **1999**, *392* (1), 77–84. [https://doi.org/https://doi.org/10.1016/S0003-2670\(99\)00195-6](https://doi.org/https://doi.org/10.1016/S0003-2670(99)00195-6).
- (32) Kanyong, P.; Davis, J. J. Homogeneous Functional Self-Assembled Monolayers: Faradaic Impedance Baseline Signal Drift Suppression for High-Sensitivity Immunosensing of C-Reactive Protein. *J. Electroanal. Chem.* **2020**, *856*, 113675. <https://doi.org/https://doi.org/10.1016/j.jelechem.2019.113675>.
- (33) Eda, S.; Kaufmann, J.; Molwitz, M.; Vorberg, E. A New Method of Measuring C-Reactive Protein, with a Low Limit of Detection, Suitable for Risk Assessment of Coronary Heart Disease. *Scand. J. Clin. Lab. Investig. Suppl.* **1999**, *59* (230), 32–35. <https://doi.org/10.3109/00365519909168324>.
- (34) Ledue, T. B.; Rifai, N. Preanalytic and Analytic Sources of Variations in C-Reactive Protein Measurement: Implications for Cardiovascular Disease Risk Assessment. *Clin. Chem.* **2003**, *49* (8), 1258 LP – 1271. <https://doi.org/10.1373/49.8.1258>.
- (35) WHO. C-Reactive Protein Concentrations as a Marker of Inflammation or Infection for Interpreting Biomarkers of Micronutrient Status. Vitamin Asn Mineral Nutrition Information System. **2014**, 1–4.
- (36) Reviews, I. L. W. Iron Status. *WHO Libr.* **2007**, *second edi* (ISBN 978924 1596107), 1–112.
- (37) Supplied, M.; Handling, S.; Notes, P.; Preparation, R.; Procedure, A.; Results, T.; Curve, T. S.; Quality, T.; Parameters, C.; Characteristics, P.; et al. Enzyme Immunoassay Kit. 1–12.
- (38) Kanyong, P.; Pemberton, R. M.; Jackson, S. K.; Hart, J. P. Development of a Sandwich Format, Amperometric Screen-Printed Uric Acid Biosensor for Urine Analysis. *Anal. Biochem.* **2012**, *428* (1), 39–43. <https://doi.org/https://doi.org/10.1016/j.ab.2012.05.027>.
- (39) Rong, Z.; Chen, F.; Jilin, Y.; Yifeng, T. A C-Reactive Protein Immunosensor Based on Platinum Nanowire / Titania Nanotube Composite Sensitized Electrochemiluminescence. *Talanta* **2019**, *205*, 120135. <https://doi.org/https://doi.org/10.1016/j.talanta.2019.120135>.
- (40) Dong, S.; Zhang, D.; Cui, H.; Huang, T. ZnO/Porous Carbon Composite from a Mixed-Ligand MOF for Ultrasensitive Electrochemical Immunosensing of C-Reactive Protein. *Sensors Actuators B Chem.* **2019**, *284*, 354–361. <https://doi.org/https://doi.org/10.1016/j.snb.2018.12.150>.

For Table of Contents Only

